

Cyclic plasticity and damage of metals by a gradient-enhanced CDM model

GiangiacoMo Minak

DIEM, Facoltà di Ingegneria, Università degli Studi di Bologna, Bologna – Italy

Fulvio E. G. Chimisso

DMC, Fundação Universidade Federal do Rio Grande, Rio Grande, RS – Brazil

Heraldo S. da Costa Mattos

DEM, Laboratório de Mecânica Teórica e Aplicada, Universidade Federal Fluminense, Niterói, RJ – Brazil

Abstract

In the present work a thermodynamically consistent mechanical model for damageable elasto-plastic materials is proposed. The governing equations are obtained within the framework of a microstructure theory since a scalar damage variable is introduced as an additional kinematic variable. The constitutive equations are developed within a thermodynamic framework taking the damage variable and also its gradient as state variables. This model leads to an adequate description of the softening behavior due to the degradation of the microstructure. The main features of the proposed theory are discussed through the simulation and the comparison with the results of low cycle fatigue tests performed on a structural aluminum alloy.

Keywords: low cycle fatigue, continuum damage mechanics, elasto-plasticity, non-local damage model, microstructure, aluminium alloy

1 Introduction

Continuum Damage Mechanics uses a phenomenological approach to model the effect of microscopic geometric discontinuities induced by the deformation process (micro-cracks, micro-voids, etc.) on the macroscopic behavior of a structure. In continuum damage theories, an internal variable related to the growth and coalescence of microscopic defects before the macroscopic crack initiation (whose definition and physical interpretation may vary from one model to the other) is introduced and the problem becomes to establish the constitutive relations for the damage variable as a function of the other state variables.

Since the increase of damage generally leads to a local softening behavior, the models based on a local approach may lead to a physically unrealistic description of strain localization phenomenon.

In general, if the simplifying hypothesis of quasi-static processes is adopted, the resulting mathematical problems may present an infinity number of solutions with discontinuous fields of displacement due to the loss of ellipticity of the governing equations in the post-localization range [1]. Besides, local theories are not able to an adequate simulation of length scale dependent problems. This leads to numerical difficulties of mesh-dependence [2–5]. Even if the fully coupled dynamic and thermo-mechanical problem is considered, the physical description of wave propagation phenomena may be unrealistic, and the existence of solution of resulting mathematical problems may not be assured. Hence, some alternative approaches to the local theories for strain-softening materials (taking into account the damage or not) have been proposed in the last years such as non-local modeling of the constitutive behavior and gradient dependent material description.

The integral non-local theories [6] make a spatial averaging of some of the variables of the problem (in the case of damage theories, a spatial averaging of the internal variable related to the damage). This regularization procedure depends on a weighting function that varies from one theory to the other.

In the theories with gradient dependent material description [7] the free energy may be a function not only of the state variables that appear in the classical local theories but also of higher order gradients of these variables. To set up a general gradient constitutive theory it is necessary to consider aspects of the second law of thermodynamics since dissipative phenomena may be taken into account. One difficulty from the theoretical point of view in these theories is to assure that the second law restriction is satisfied in all processes. When only higher order deformation gradients are considered in the free energy function this problem is affordable, but when gradients of the internal variables are taken into account it is not easy to verify whether the constitutive theory is thermodynamically admissible or not. A particular case of the gradient theories that overcome this difficulty is when the continuum possesses a substructure or microstructure. Since the pioneer work of E. and F. Cosserat (1909) [8], theories of continua with microstructures have been proposed as an alternative approach to many complex physical problems [9–21] and a general discussion about such kind of theory can be found in many of these references. In all these theories, in order to account for the microstructure, a reformulation of the kinematics (to include the possible microscopic motions) and of some basic governing principles of the classical Continuum Mechanics is necessary.

In the present paper it is discussed the possibility of low cycle fatigue prediction through a continuum damage theory in which the material is considered to possess a substructure or microstructure. This kind of approach has been adopted in the last years by a few different groups and very promising results were obtained up to now [19, 22–26]. A thermodynamically consistent damage theory developed within this framework is presented. It enables a convenient macroscopic (phenomenological) description of the degradation induced by the deformation process. This theory of continuum media with microstructure is developed from formal arguments of Continuum Mechanics what makes easier the choice of the free energy and, consequently, the development of physically realistic constitutive equations. The main feature is that the additional “degree of freedom” related to the microscopic motions is not a microrotation as in the micropolar continuum theories [16] but a damage scalar variable related

with the links between material points. An additional balance equation is included to account for the microscopic forces related to this variable. Besides, the free energy is supposed to be a function not only of this variable, but also of its gradient. The theory enables a convenient macroscopic (phenomenological) description of the degradation induced by the deformation process accounting for the strain-softening and localization behaviors. The main features of such kind of approach are discussed performing simulations of low cycle fatigue tests on metallic bars. The parameters used in the simulation are the ones of an AA 2011 aluminum alloy, identified by static and cyclic tests. The results of the simulations in terms of hysteresis loop shape and fatigue life are compared.

2 Mathematical model

2.1 Preliminary definitions and summary of the basic balance equations

In this section we postulate appropriate conservation laws that govern the evolution of a continuous damageable body which is defined as a set of material points \mathbf{B} which occupies a region Ω of the Euclidean space at the reference configuration. For the sake of simplicity the hypothesis of small deformation will be assumed throughout this work. Hence, the density ρ is assumed to be constant in time and the conservation of mass principle is automatically satisfied.

In this theory, besides the classical variables that characterize the kinematics of a continuum medium (displacements, velocities and accelerations of material points), an additional variable $\beta \in [0,1]$ is introduced. A point, in such continuum theory, is representative of a given “volume element” of the real material and it is endowed with a microstructure that accounts for the kinetic energy and internal power of the microscopic motions associated to the microscopic geometric discontinuities (density of micro-cracks or cavities). This variable is related with the microscopic motions and can be interpreted as a measure of the damage state of the “volume element”. If $\beta=1$, all the links between material points are preserved and the initial material properties are also preserved. If $\beta=0$, a local rupture is considered. When $\beta=1$, the kinetic energy associated with the microscopic motions and also the power of the microscopic forces are equal to zero in the “volume element”. Since the degradation is an irreversible phenomenon, the variation rate $\dot{\beta}$ must be negative or equal to zero.

A conservation law for the microscopic forces associated to β is postulated here. The proposed principles have been briefly presented in [20] and may be regarded as a special case of the theories of continuum with microstructure ([10, 11], for instance). In particular these governing principles are very close to those proposed in the theory of elastic materials with voids [13]. Nevertheless, the definition and the physical interpretation of the additional kinematic variable and also the proposed constitutive equations make both theories very different. In the theory of elastic materials with voids the additional variable is related with the change in solid volume fraction. The present theory assumes that the damage is related with micro-cracks and not with micro-voids, and hence the damaged material is not considered a porous medium and the damage variable is not directly related with a volume change. The difference between these different kinds of geometric discontinuities at the microscopic level are more evident when large deformations, heat transfer or wave propagation are considered.

The necessary thermal and mechanics fields variables are introduced as primitive quantities. Specifically, there exists a density $\rho : \Omega \rightarrow R$, a stress tensor $\underline{\sigma} : \Omega \rightarrow M^3$, a body force $\underline{b} : \Omega \rightarrow R^3$, a specific internal energy $e : \Omega \rightarrow R$, a heat flux vector $\underline{q} : \Omega \rightarrow R^3$, a specific entropy $s : \Omega \rightarrow R$ and a temperature $\theta : \Omega \rightarrow R$. In addition, we introduce a microscopic stress vector $\underline{H} : \Omega \rightarrow R^3$, a microscopic internal force $M : \Omega \rightarrow R$ and a microscopic distant force $y : \Omega \rightarrow R$. In this work an arbitrary part \mathbf{P} of the body \mathbf{B} that occupies a region $R \subset \Omega$ at the reference configuration is taken as a mechanical system. By definition, the boundary of the region R will be called. Besides the classical balance relations for mass, linear momentum and angular momentum the evolution of the damageable body us governed by the following balance relations:

Balance of microscopic forces:

$$\frac{d}{dt} \int_R (\rho l \beta) = \int_{\Gamma} (\underline{H} \cdot \underline{n}) + \int_R (y - M); \quad \forall R \subset \Omega \quad (1)$$

The term l in equation (1) is called the equilibrated inertia. It can be shown [20] that l is such that $\dot{l} = 0$. In some basic works concerned with microstructure theories ([27], for instance), the microscopic inertia term ρl is considered in the balance of microscopic forces. The role of l in the present theory is controversial due to the particular definition of β . Since the hypothesis of quasi-static evolution is adopted in all the examples presented in this paper the role of the microscopic inertia is not discussed in the analysis. The microscopic external force y must be introduces in the theory in order to take into account the non mechanical actions (chemic of electromagnetic) that affect the damage state of the material even if there is no mechanical deformation. The role of such kind of external microscopic force is discussed in [18]. In the present paper it is assumed, in all examples, that $y = 0$.

Balance of energy:

$$\frac{d}{dt} \int_R \left[\rho \left(e + \frac{1}{2} \dot{\underline{u}} \cdot \dot{\underline{u}} + \frac{1}{2} l \beta^2 \right) \right] = \int_{\Gamma} \left[(\underline{\sigma} \dot{\underline{u}} + \underline{H} \dot{\beta} - \underline{q}) \cdot \underline{n} \right] + \int_R (\underline{b} \cdot \dot{\underline{u}} + y \beta); \quad \forall R \subset \Omega \quad (2)$$

Second law of thermodynamics:

$$\frac{d}{dt} \int_R (\rho s) \geq - \int_{\Gamma} \frac{\underline{q} \cdot \underline{n}}{\theta}; \quad \forall R \subset \Omega \quad (3)$$

The variable $\dot{\underline{u}}$ is the time derivative of the displacement \underline{u} . After some manipulation, the expressions(1), (2) and (3) lead, respectively to the local forms:

$$-M + \text{div} \underline{H} + y = \rho l \ddot{\beta} \quad (4)$$

$$\rho \dot{e} = -\text{div} \underline{q} + \underline{\sigma} : \nabla \dot{\underline{u}} + \underline{H} \cdot \nabla \dot{\beta} + M \dot{\beta} \quad (5)$$

$$\rho \theta \dot{s} = \text{div} \underline{q} - \frac{1}{\theta} \underline{q} \cdot \nabla \theta \geq 0 \quad (6)$$

An alternative local form for the second law of thermodynamics (which will be useful later) can be obtained by the substitution of expression (5) in (6) and the introduction of the free energy:

$$\psi = e - \theta s \quad (7)$$

giving rise to the inequality:

$$d = \underline{\underline{\sigma}} : \dot{\varepsilon} + \underline{\underline{H}} \cdot \nabla \dot{\beta} + M \dot{\beta} - \rho \left(\dot{\psi} + s \dot{\theta} \right) - \frac{1}{\theta} \underline{\underline{q}} \cdot \nabla \theta \geq 0 \quad (8)$$

where $\varepsilon = \frac{1}{2} \left(\nabla u + (\nabla u)^T \right)$ is the local strain. The expression (8) defines the rate of energy dissipation d and can be interpreted as the Clausius-Duhem inequality for this kind of continuum under the assumption of small deformations (which takes into account the power of the microscopic internal forces $\left(\underline{\underline{H}} \cdot \nabla \dot{\beta} + M \dot{\beta} \right)$).

2.2 Constitutive equations

The fundamental principles presented in the previous section are valid for any kind of damageable body. In this section, we restrict ourselves to elasto-plastic behavior and isothermal processes. The theory can be summarized in the four steps below.

a) State variables

Under the hypothesis of small deformations and isothermal processes, the local state of a elasto-plastic material is supposed to be a function of the total strain ε , of the plastic strain ε^p , of the damage variable β , of its gradient $\nabla \beta$ and also of a scalar variable p associated to the isotropic hardening and of a second order tensor variable associated with the kinematic hardening.

b) Free energy – state laws

Following the classical assumption of Thermodynamic of Irreversible Processes, the free energy is supposed to be a function of the state variables. Thus, the following expression is proposed for the free energy:

$$\psi(\varepsilon, \varepsilon^p, c, p, \beta, \nabla \beta) = \beta [\psi_e(\varepsilon - \varepsilon^p) + \psi_p(p) + \psi_c(c)] + \frac{1}{2} k (\nabla \beta \cdot \nabla \beta) \quad (9)$$

with

$$\psi_e = \frac{E}{2(1+\nu)} \left\{ \frac{\nu}{1-2\nu} [tr(\varepsilon - \varepsilon^p)]^2 + (\varepsilon - \varepsilon^p) \cdot (\varepsilon - \varepsilon^p) \right\} \quad (10)$$

$$\psi_p = v_1 [p + \exp(-v_2 p)] + p \sigma_y \quad (11)$$

$$\psi_c = \frac{1}{2} a (c \cdot c) \quad (12)$$

where E is the Young modulus, ν is the Poisson's ratio, k , v_1 , v_2 and a are positive constants and $\varepsilon = (\varepsilon - \varepsilon^p)$ is the elastic strain tensor. The term $\frac{1}{2} k (\nabla \beta \cdot \nabla \beta)$ is considered so as to give to β a diffusive behavior, thus smoothing the field β in Ω .

The here called thermodynamic forces $(\underline{\sigma}, \underline{x}, y, G, \underline{H})$, related to the state variables $(\underline{\varepsilon}, \underline{c}, p, \beta, \nabla\beta)$, are defined from the free energy by the state laws:

$$\underline{\sigma} = \frac{\partial\psi}{\partial\underline{\varepsilon}^p} = \frac{\beta E}{1+\nu} \left[\frac{\nu}{1-2\nu} \text{tr}(\underline{\varepsilon} - \underline{\varepsilon}^p)^2 + (\underline{\varepsilon} - \underline{\varepsilon}^p)^2 : (\underline{\varepsilon} - \underline{\varepsilon}^p)^2 \right] \quad (13)$$

$$\underline{x} = \frac{\partial\psi}{\partial\underline{c}} = \beta(a\underline{c}) \quad (14)$$

$$y = \frac{\partial\psi}{\partial p} = \beta [v_1(1 - \exp(-v_2 p)) + \sigma_y] \quad (15)$$

$$G = \frac{\partial\psi}{\partial\beta} = \psi_e + \psi_p + \psi_c \quad (16)$$

$$\underline{H} = \frac{\partial\psi}{\partial\nabla\beta} = k\nabla\beta \quad (17)$$

To complete the constitutive equations, additional information about the dissipative behavior must be given. This information can be obtained from a plastic potential F and are called the evolution laws.

c) Plastic potential – evolution laws

The potential F is presumed to have the form:

$$F = J(\underline{\sigma} - \underline{x}) - y + g(\underline{x}, G; \underline{\varepsilon}, \underline{\varepsilon}^p, p, \underline{c}, \beta) \leq 0$$

with $J(\underline{\sigma} - \underline{x})$ being von Mises equivalent stress: $J(\underline{\sigma} - \underline{x}) = \left[\frac{3}{2}(\underline{\sigma} - \underline{x})_{dev} : (\underline{\sigma} - \underline{x})_{dev} \right]^{1/2}$ and $g = \frac{b}{2a}(\underline{x} : \underline{x}) - \frac{ab}{2}(\beta^2 \underline{c} : \underline{c}) + \frac{G^2}{2S_0} - \frac{1}{2S_0}(\psi_e + \psi_p + \psi_c)^2$ a dissipative term. σ_y is the yielding stress.

Together with the plastic potential F , another potential, $\hat{F}(\dot{\beta}) = \dot{\beta}$, is utilized to account for the condition $\dot{\beta} \leq 0$.

The following evolution relations are postulated:

$$\underline{\dot{\varepsilon}}^p = \lambda \frac{\partial F}{\partial \underline{\sigma}} = \lambda \frac{\frac{3}{2}(\underline{\sigma} - \underline{x})_{dev}}{J(\underline{\sigma} - \underline{x})} \quad (18)$$

$$\underline{\dot{c}} = -\lambda \frac{\partial F}{\partial \underline{x}} = \underline{\dot{\varepsilon}}^p - \frac{b}{a} \underline{x} \lambda \quad (19)$$

$$\dot{p} = -\lambda \frac{\partial F}{\partial y} = \lambda \quad (20)$$

and

$$\dot{\beta} = M - \lambda \frac{\partial F}{\partial G} - \hat{\lambda} \frac{\partial \hat{F}}{\partial \dot{\beta}} = M - \frac{\lambda(\psi_e + \psi_p + \psi_c)}{S_0} - \hat{\lambda} \quad (21)$$

The expressions from (18) to (21) are the set of evolution laws of the dissipative process, where

$$\lambda \geq 0, \quad F \leq 0, \quad \lambda F = 0 \quad \text{and} \quad \hat{\lambda} \geq 0, \quad \hat{F} \leq 0, \quad \hat{\lambda} \hat{F} = 0.$$

M is the microscopic internal force associated with β , λ is the Lagrange multiplier associated with the condition $F \leq 0$, and $\hat{\lambda}$ is the Lagrange multiplier associated with the condition $\hat{F} \leq 0$.

It can be proved [18] that, together with the evolution laws, the state laws define a complete set of constitutive equations thermodynamically admissible.

Introducing equation (17) and (21) in(4), the following balance equation is obtained

$$\dot{\beta} = k \Delta\beta - \frac{\lambda(\psi_e + \psi_p + \psi_c)}{S_0} - \hat{\lambda} \quad (22)$$

Introducing damage variable: $D = 1 - \beta$, the following expression can be derived

$$\dot{D} = k \Delta D + \frac{\lambda(\psi_e + \psi_p + \psi_c)}{S_0} + \hat{\lambda} = \left\langle k \Delta D + \frac{\lambda(\psi_e + \psi_p + \psi_c)}{S_0} \right\rangle \quad (23)$$

where $\langle n \rangle = \max\{0, n\}$. It is interesting to use D instead of β because the definition this variable is closer to the one usually adopted in the traditional works of continuum damage mechanics.

Equations (13)-(17) and (18)-(21) form a complete set of constitutive equation. Eventually, some of the material parameters should be supposed to be functions of the invariants of some of the internal variables [18]. In these cases, generally the parameter must be a function of a “maximum strain amplitude”, defined as $\max_t \left\{ J(\underline{\underline{\varepsilon}}^p(t)) = \left[\frac{3}{2} (\underline{\underline{\varepsilon}}^p(t))_{dev} : (\underline{\underline{\varepsilon}}^p(t))_{dev} \right]^{1/2} \right\}$ Chimisso, 1994.

These constitutive equations, in its evolutionary form, simplified and reduced for the one-dimensional case, are presented below. In the present paper, the examples are restricted to a one-dimensional context in order to analyze how to identify the different parameters that appear in the theory. For a round bar submitted to a one-dimensional loading such that a push-pull low cycle fatigue test, the state law equations and the evolution law equations are reduced in the following (evolutive) form:

$$\dot{\sigma} = (1 - D)E(\dot{\varepsilon} - \dot{\varepsilon}^p) - \dot{D}E(\varepsilon - \varepsilon^p) \quad (24)$$

$$\dot{x} = (1 - D)(a\dot{\varepsilon}^p - b\lambda x) - \dot{D}ax \quad (25)$$

$$\dot{y} = (1 - D)v_1v_2e^{-v_2p}\dot{p} - \dot{D}[v_1(1 - e^{-v_2p}) + \sigma_y] \quad (26)$$

$$\dot{\varepsilon}^p = \lambda \frac{\sigma - x}{|\sigma - x|} \quad (27)$$

$$\dot{p} = \lambda \quad (28)$$

$$\dot{c} = \dot{\varepsilon}^p - \frac{b}{a}\lambda x \quad (29)$$

$$\dot{D} = \left\langle \frac{\lambda}{2S_0} \left\{ E(\varepsilon - \varepsilon^p)^2 + ac^2 + 2 \left[v_1 \left(p + \frac{e^{-v_2p}}{v_2} \right) + p\sigma_y \right] \right\} + k \frac{\partial^2 D}{\partial z^2} \right\rangle \quad (30)$$

where $\langle n \rangle = \max(0, n)$ and λ is the Lagrange multiplier: $\lambda \geq 0, F \leq 0, \lambda F = 0$

It is considered an initially undeformed bar, clamped and with prescribed axial displacements at the extremities. The boundary conditions are

$$u(z = 0, t) = 0, u(z = L, t) = 0; D(z = 0, t) = D(z = L, t) = 0 \text{ and the initial conditions are}$$

$$\varepsilon^p(z, t = 0) = p(z, t = 0) = c(z, t = 0) = D(z, t = 0) = D_0(z)$$

The choice of $D_0(z)$ will depend on possible presence of a flaw. For a bar without flaws we have: $D_0(z)=0$.

3 Material and experimental methods

3.1 Material

The material considered is an AA 2011 aluminium alloy heat treated T6, and its chemical composition is shown in table 1.

Table 1: Chemical composition

	Si	Fe	Cu	Mn	Mg	Cr	Zn	Ni	Ti	Pb	Bi
AA 2011	0.18	0.24	5.15	0.04	0.04	0.006	0.024	0.005	0.020	0.32	0.22

The most important element is copper, but magnesium, silica, manganese can be present. Copper, alone or associated with magnesium, gives good mechanical properties and makes the alloy suitable for heat treatment. High temperature mechanical properties are also improved, even if corrosion resistance is sensibly reduced. Another important characteristic of this class of alloys is the high value of the fracture toughness.

3.2 Methodology

Specimens were cut from an extruded bar. Fatigue test specimens were precision machined from the bar using a numerical-control lathe. The specimens were machined with the stress axis parallel to the extrusion direction.

They were smooth and cylindrical in the gauge section, which measured 12 mm in diameter and 25 mm in length. The length to diameter ratio of the fatigue specimens was chosen to ensure that it would not buckle during the fully reversed cyclic training.

The machined surface did not need any further polishing since no circumferential scratches or surface machining marks were present. The experimental tests have been carried out by means of a servo hydraulic Instron 8032 machine equipped with a 100 KN dynamical load cell and dynamical clip-on extensometer with a gage length of 25 mm.

Quasi-static tests to determine Elastic modulus and Yield strength were performed in displacement control using as input a ramp with a rate of 0.01 mm/s.

Strain controlled low cycle fatigue tests were carried out in tension-compression with a load ratio $R=-1$ according to ASTM E 606 standard method. The frequency utilized in the fatigue tests was 0.1 Hz, to obtain an isotherm process, and the imposed load wave shape was triangular. The total number of specimen tested in this configuration was nine.

The ASTM standard test method provides parameters for the definition of failure of the tested specimen: the percent reduction of the applied load or the presence of a macroscopic crack on the specimen surface. However, the alloy does not show any softening before failure, so the monitoring of the percent reduction of the applied load is not a suitable parameter for evaluating damage.

To identify surface cracks is an even more difficult task since the defect appears in different ways, depending on the strain level and on the material; furthermore the cracks do not always start on the surface, but also in the inner part. A sharp variation of the dynamic stiffness, calculated for every cycle from the load cell and extensometer data, was therefore taken as the failure condition. In fact this variation is a symptom of the presence of a macroscopic crack. The variation is not always represented by a reduction, but sometimes it may appear as an increase.

This, as verified *a posteriori*, depends upon the point from which the crack starts. In fact, the crack usually originates on the surface, but, even if it is certainly between the extensometer blades, its circumferential position determines either an apparent increasing or decreasing of the specimen stiffness. The section is no longer symmetrical with respect to the load and a flexural stress appears. The neutral axis does not coincide with the specimen axis, but rather it moves toward the extensometer which, as a consequence, undergoes less strain with respect to the undamaged specimen case. The specimen appears to be more rigid and consequently the dynamic elastic modulus increases. Vice versa, in the case of a crack originating from a point between the extensometer blades, the measured strain is higher, the specimen appears less stiff and a decreasing dynamic elastic modulus is found.

The loss of loop stability (as seen in figure 1) is another criterion for stopping the test.

Load, displacement and strain were acquired by means of a National Instrument DAQ board and a virtual instrument was created in LabView® 6.0.

To assure load alignment on the specimen, before each test, the strain measured by means of four strain gages glued to the median plane of the specimen were verified to be compatible to pure membrane strain condition. Four strain gages were glued to an unloaded specimen for thermal compensation and the final electrical configuration was composed by two full bridges, each one containing two active strain gages located on the same diameter of the specimen and connected in order to eliminate membrane strain and sum flexural strains.

4 Results

4.1 Material properties

In table 2 are reported the mean values of the ultimate and yield stress, of the strain to failure, the elastic modulus and the Brinell hardness.

In figure 2 the cyclic curve and the first part of the quasi-static stress-strain curve are compared: the hardening behaviour due to cyclic load is evident.

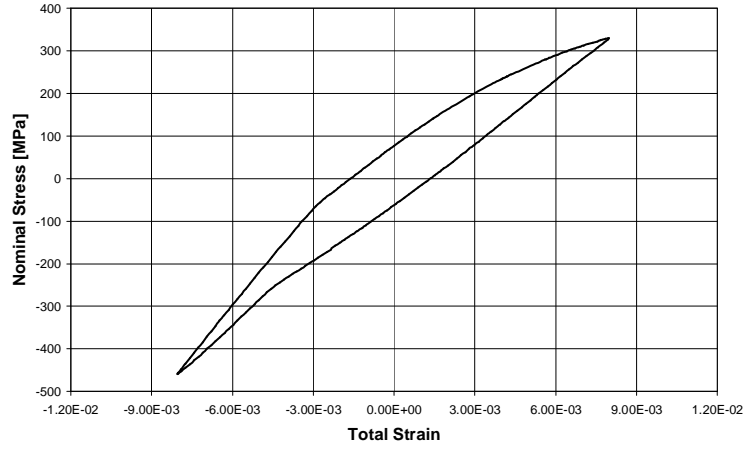


Figure 1: Loop instability due to a macroscopic crack

Table 2: Measured mechanical properties

	σ_u [MPa]	σ_y [MPa]	All.%	E [GPa]	HRB
AA 2011	403	280	34.5%	74	70.7

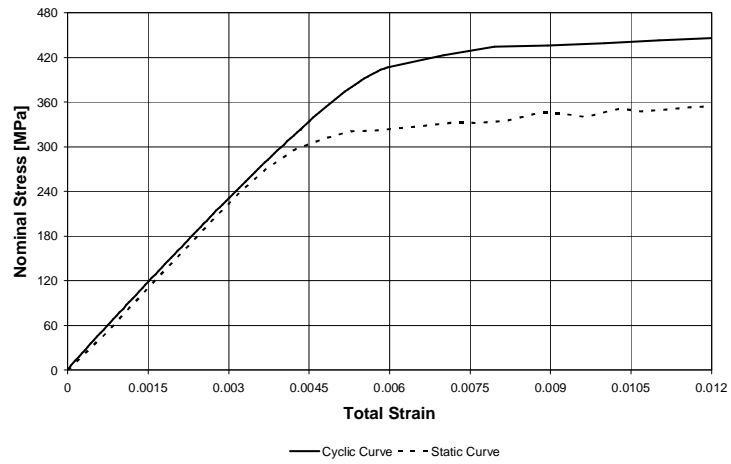


Figure 2: Cyclic and quasi-static curve for the AA 2011 alloy

4.2 Model parameters identification

The hysteresis loop was acquired by means of an *ad hoc* virtual instrument and the parameters were determined for each cycle, not just for the stabilized one.

To calculate the parameters related to kinematic hardening, the makes use of a classic procedure, as shown in figure 3, for the plastic arc extraction.

For the decreasing part of the loop the point P1 is determined by the change of slope in an elastic-perfectly plastic model and P2 is the symmetric point in the increasing part.

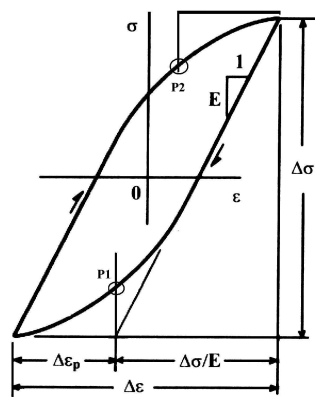


Figure 3: Plastic arc extraction

The arcs thus obtained are interpolated using the techniques described in [28], by means of the equation (31) where the parameters are those appearing in the kinematic hardening model (25). For the determination of isotropic hardening parameters the maximum stress is plotted as a function of the accumulated plastic strain. In our model v_1 is obtained from the asymptotic behaviour of the curve, while v_2 is derived from the transient behaviour, as appears evident from the equation (32) derived from (26).

$$x = \frac{a}{b} + c \cdot e^{-b\varepsilon_p} \quad (31)$$

$$y = S_y + v_1 (1 - e^{-v_2 p}) \quad (32)$$

Figure 4 shows maximum stress as a function of accumulated plastic strain.

The strain controlled tests show that the isotropic hardening parameters values are $v_1=112$ MPa and $v_2=10.8$ constant and independent from the strain level. On the contrary, all the other parameters were found to be strain level dependent.

In figure 5, as an example, the trend of the parameter a of the kinematic hardening for the 1.2% strain level is shown. As can be easily seen, the value of the parameter stabilizes rather quickly.

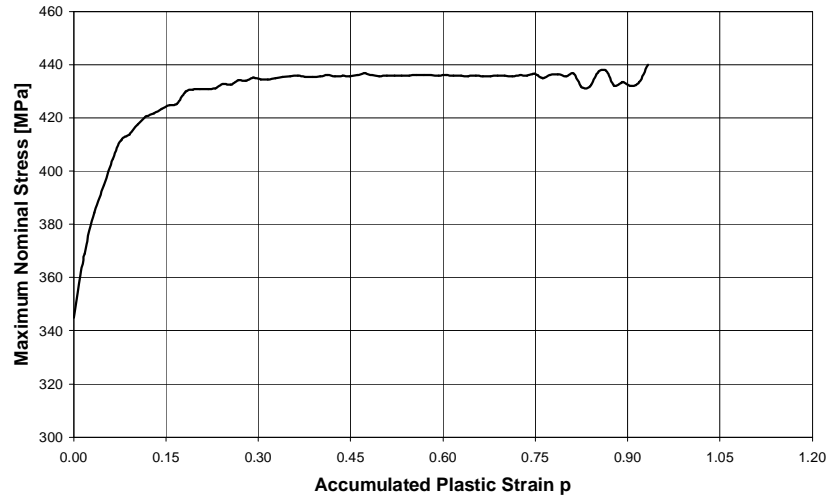
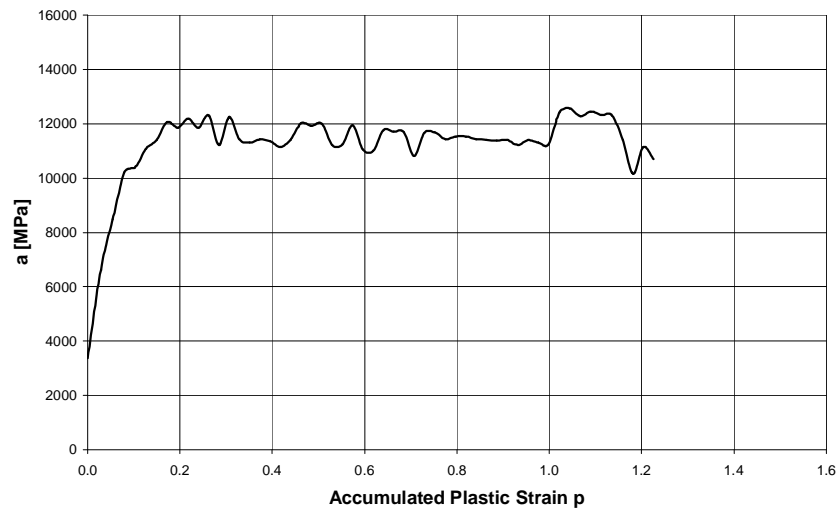


Figure 4: Isotropic hardening

Figure 5: Trend of the parameter a , strain level $\pm 1.2\%$

The trends of the kinematic hardening parameters a and b , calculated for the stable hysteresis loop for each strain level, are shown in figures 6a and 6b in logarithmic coordinates. The trend for the damage parameter S_o is shown in figures 6c.

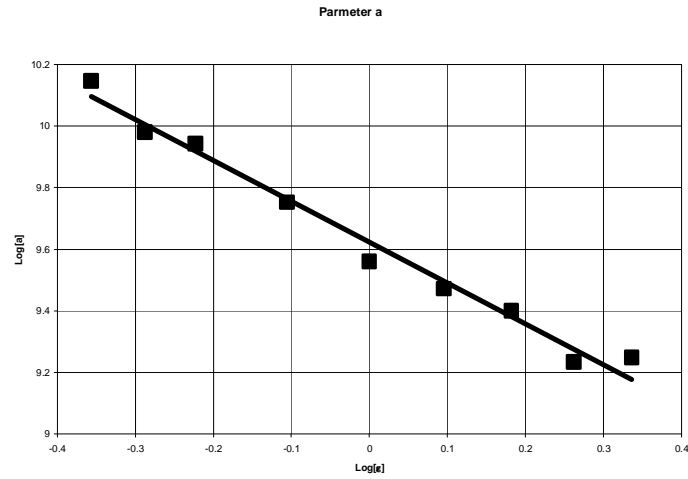


Figure 6a: Trend for the parameter a

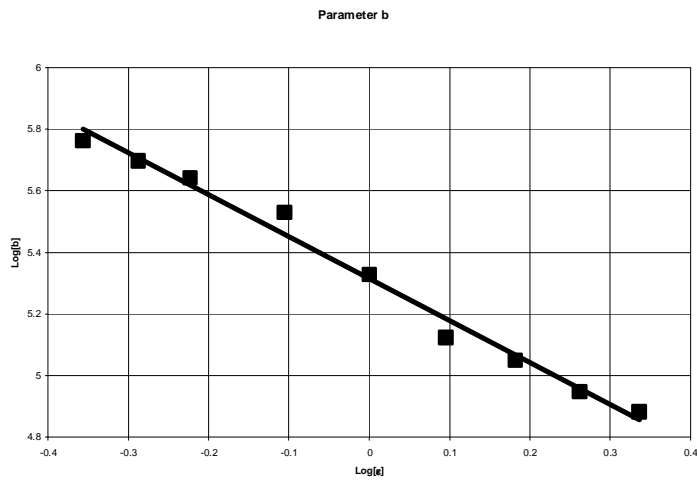
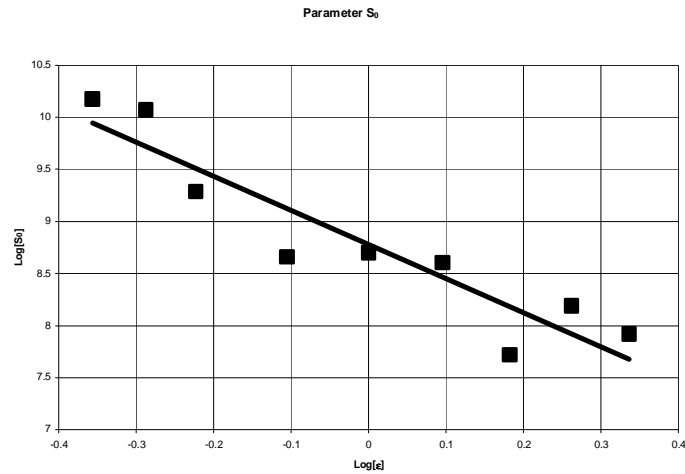
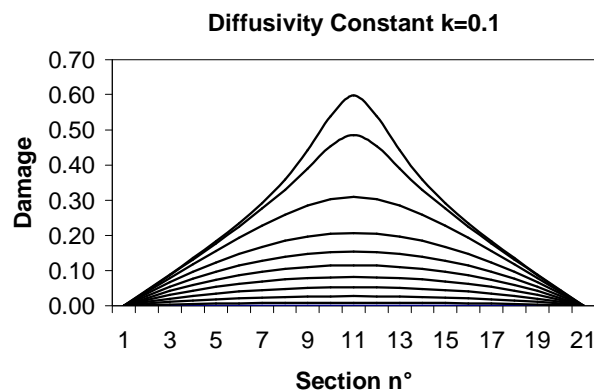
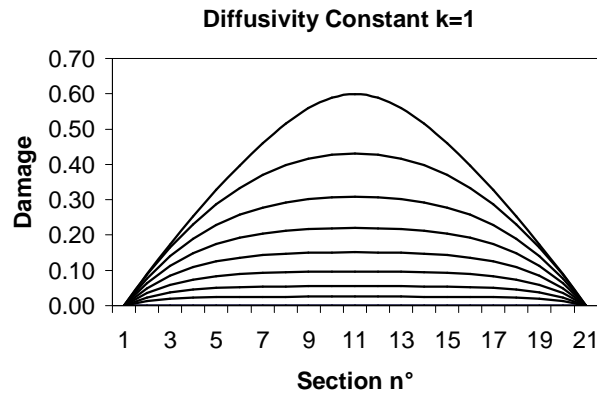
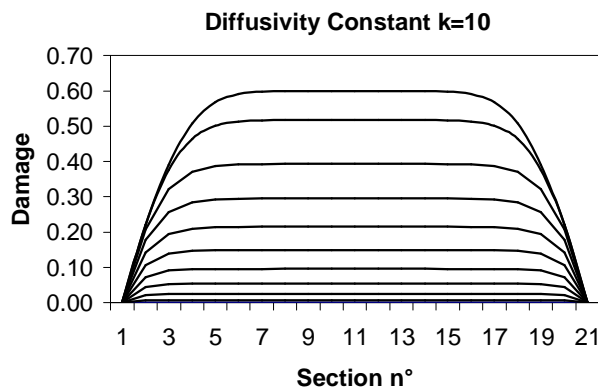


Figure 6b: Trend for the parameter b

Figure 6c: Trend for the parameter S_0

To appreciate the effect of the damage diffusion, figures 7a,b, and c, show as an example the damage distribution along the specimen for three different values of k . In each graph the different curves represent damage evolution at different increasing cycle numbers. It can be noted that the lower the value of the parameter, the more the damage tends to concentrate in the median section of the specimen. For high values of k damage is nearly constant over the specimen length. The failure mode of the specimens is much localized so a suitable value for the damage diffusion parameter k was chosen to be 0.1.

Figure 7a: $k=0.1$, damage along the specimen at different cycles number

Figure 7b: $k=1$, damage along the specimen at different cycles numberFigure 7c: $k=10$, damage along the specimen at different cycles number

The analytic expressions of the parameters are the following:

$$a = 15.12 \left(\frac{\Delta \varepsilon}{2} \right)^{-1.326} \quad (33a)$$

$$b = 0.203 \left(\frac{\Delta \varepsilon}{2} \right)^{-1.359} \quad (33b)$$

$$S_0 = 649 \left(\frac{\Delta \varepsilon}{2} \right)^{-3.278} \quad (33c)$$

These interpolating functions are defined by two parameters, a coefficient and an exponent, so the minimum number of specimens needed for the evaluation of the trends is two.

We calculated the parameters using different sets of two or three specimens and did the simulation for each case.

We defined an index to rank the solutions as:

$$Q = \frac{\sum_{i+1}^{n_{spec}} (N - N_{exp})^2}{\sum_{i+1}^{n_{spec}} (N_{rs} - N_{exp})^2} \quad (34)$$

Where N is the number of cycles calculated in the present simulation, N_{exp} is the number of cycles found experimentally and N_{rs} is the number of cycles evaluated in the reference simulation (obtained using the formulas 33a,b,c). The higher the values of this index, the worse the solution.

In figure 8 it is plotted the value of Q as a function of the distance of the specimens in terms of strain range. In the case of three specimens the third was always the median of the other two.

It is possible to see that the two specimen set gives good results only if the difference in the strain levels is high, while using the three specimens set very good solutions are found if the strain range difference is not too small.

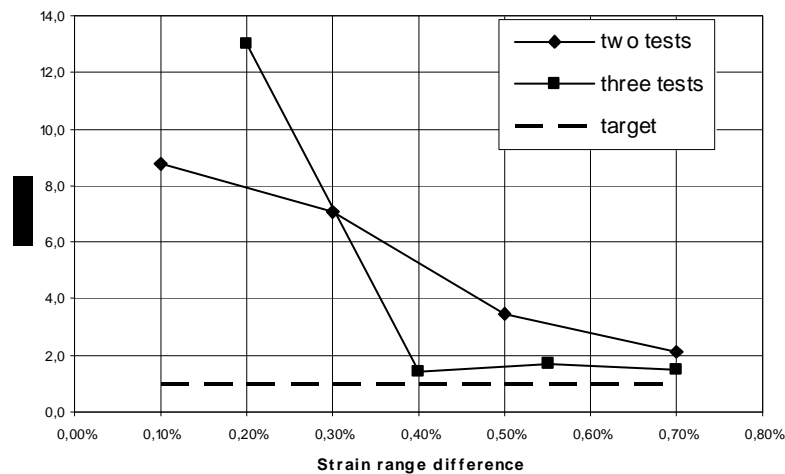


Figure 8: Index Q as a function of the strain range difference

So it is possible to conclude that a set of three specimens can be used to evaluate the parameters trend.

In figures 9a,b as an example it is possible to see the trends of the dynamic elastic modulus as a function of the number of cycles. It is worth noticing that in one case there is an apparent stiffness

increase, while in the other case the stiffness decreases due to a crack arising from the opposite side with respect to the extensometer position.

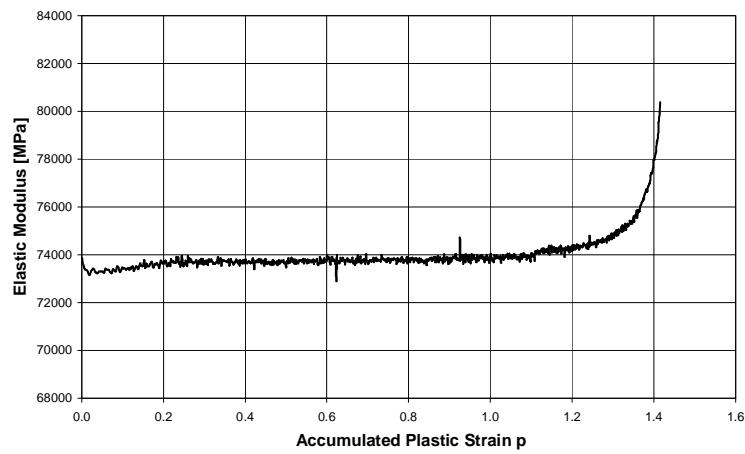


Figure 9a: Dynamic elastic modulus, strain level $\pm 0.6\%$

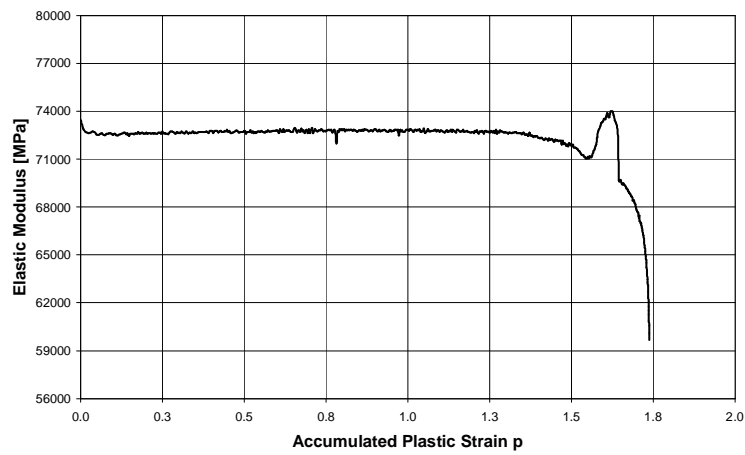


Figure 9b: Dynamic Elastic Modulus, Strain level $\pm 0.65\%$

4.3 Validation of the model

To validate the model the parameters trends identified using three specimens loaded at three different ($\pm 0.6\%$, $\pm 1\%$, $\pm 1.4\%$) total strain levels were utilized. In figure 10 for a typical stabilized cycle a modelled cycle is compared with the real one. The strain level is 1.2%, not used for the parameter identification, nevertheless a very good agreement is evident

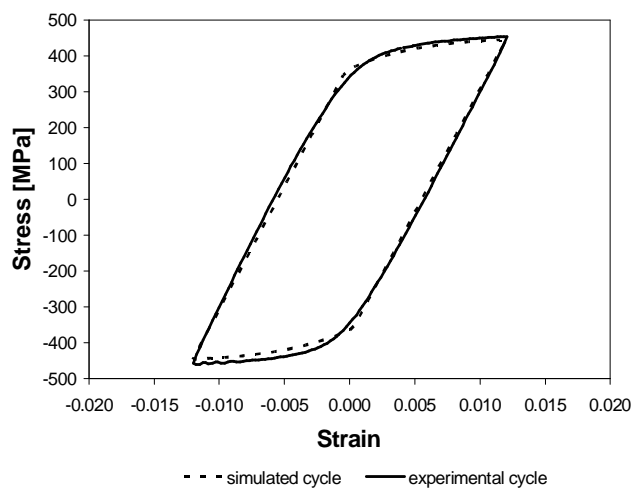


Figure 10: Real and modelled cycle, strain level 1.2%

In figure 11 are shown the experimental data, the Manson-Coffin interpolation curve and the simulated data.

The results are quite satisfactory and the simulated data are closer to the Manson-Coffin curve than the experimental data due to the experimental errors averaging.

5 Conclusions

This paper proposes a consistent framework in which to model the fatigue of elasto-plastic materials. The theory allows an adequate description of the strain localization phenomenon induced by the damage. The numerical results show that this theory is a promising tool in the analysis of low cycle fatigue in metallic materials.

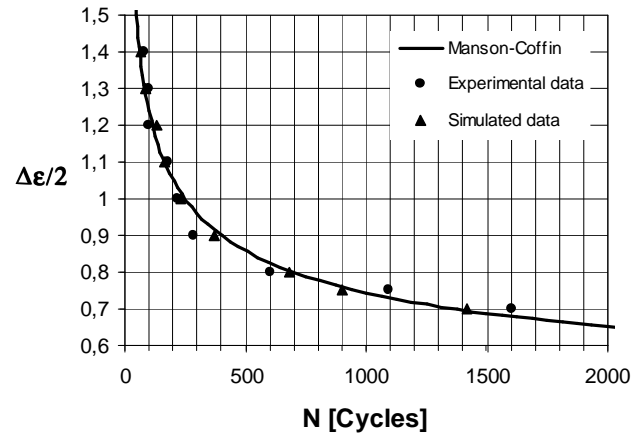


Figure 11: Fatigue life curve

References

- [1] Needleman, A., Material rate dependence and mesh sensitivity in localization problems. *Comput Meth Appl Mech Eng*, **67**, pp. 69–87, 1988.
- [2] Knowles, J. & Sternberg, E., On the failure of ellipticity and the emergence of discontinuous deformation gradients in plane finite elastostatics. *J Elasticity*, **8**, pp. 329–379, 1978.
- [3] Pietruszczak, S. & Mroz, Z., Finite element analysis of the deformation of strain-softening materials. *Int J Numer Meth Eng*, **17(327-334)**, 1981.
- [4] Bazant, Z. & Cabot, G., Nonlocal continuum damage, localization, instability and convergence. *ASME J Appl Mech*, **55**, pp. 287–293, 1988.
- [5] Vree, J.D., Brekelmans, W., Vree, M.V.G.D., Brekelmans, W. & Gils, M.V., Comparison of nonlocal approaches in continuum damage mechanics. *Comp & Struct*, **55**, pp. 581–588, 1995.
- [6] Bazant, Z. & Cedolin, L., *Stability of structures - Elastic, inelastic and damage theories*. Oxford University Press, 1991.
- [7] Benallal, A. & Tvergaard, V., Nonlocal continuum effects on bifurcation in the plane strain tension-compression test. *J Mech Phys Solids*, **43(5)**, pp. 741–770, 1995.
- [8] Cosserat, E. & Cosserat, F., *Théorie des Corps Déformables*. Herman et Fils: Paris, 1909.
- [9] Green, A. & Rivlin, R., Simple force stress multipoles. *Arch Rat Mech Anal*, **16**, pp. 23–353, 1963.
- [10] Mindlin, R., Microstructure in linear elasticity. *Arch Rat Mech Anal*, **16(51-78)**, 1964.
- [11] Toupin, R., Theories of elasticity with couple-stress. *Arch Rat Mech Anal*, **17(85-112)**, 1964.
- [12] Kafadar, C. & Eringen, A., Micropolar media - i, the classical theory. *Int J Eng Sci*, **9(3)**, pp. 271–305, 1971.
- [13] Cowin, S. & Nunziato, J., Linear materials with voids. *J of Elasticity*, **13**, pp. 125–147, 1983.
- [14] Mattos, H.C., Fremond, M. & Mamiya, E., A thermodynamically consistent mechanical model for damaging elastic materials. Internal report, Instituto Politécnico do Rio de Janeiro, 1990.
- [15] Mattos, H.C., Fremond, M. & Mamiya, E., A simple model of the mechanical behavior of ceramic-like

- materials. *Int J Solids Structures*, **24**, pp. 3185–3200, 1992.
- [16] Borst, R.D., Simulation of strain localization: A reappraisal of the cosserat continuum. *Eng Computations*, **8**, pp. 317–332, 1991.
- [17] Fleck, N. & Hutchinson, J.W., A phenomenological theory of strain gradient plasticity. *J Mech Phys Solids*, **41**, pp. 1825–1857, 1993.
- [18] Chimento, F., *A Continuum damage model for materials with elasto - plastic behavior*. Ph.D. thesis, Department of Mechanical Engineering, Pontifícia Universidade Católica do Rio de Janeiro, Rio de Janeiro, 1994. (In Portuguese).
- [19] Chimento, F. & Mattos, H.C., Modeling the softening behavior of damageable elasto-plastic bars. *Localized Damage III. Computer Aided Assessment and Control.*, eds. M. Aliabadi, A. Carpinteri, S. Kaliszky & D. Cartwright, Computational Mechanics Publication, 1994.
- [20] Mattos, H.C. & Sampaio, R., Analysis of the fracture of brittle elastic materials using a continuum damage model. *Structural Engineering and Mechanics*, **3(5)**, pp. 411–427, 1995.
- [21] Fremond, M. & Nedjar, B., Damage, gradient of damage and principle of virtual power. *Int J Solids Structures*, **33(8)**, pp. 1083–1103, 1996.
- [22] Bonora, N., A non linear cdm model for ductile failure. *Engineering Fracture Mechanics*, **58(I/2)**, pp. 11–28, 1997.
- [23] Bonora, N. & Newaz, G., Low cycle fatigue life estimation for ductile metals using a non linear continuum damage mechanics model. *Int J Solids Structures*, **35(16)**, pp. 1881–1894, 1998.
- [24] Nedjar, B., Elastoplastic-damage modeling including the gradient of damage: formulation and computational aspects. *International Journal of Solids and Structures*, **38**, pp. 5421–5451, 2001.
- [25] Pirondi, A. & Bonora, N., Modeling ductile damage under fully reversed cycling. *Computational Materials Science*, **26**, pp. 129–141, 2003.
- [26] Steglich, D., Pirondi, A., Bonora, N. & Brocks, W., Micromechanical modeling of cyclic plasticity incorporating damage. *International Journal of Solids and Structures*, **42(337-351)**, 2005.
- [27] Goodman, M. & Cowin, S., A continuum theory for granular materials. *Arch Rational Mech Anal*, **44**, pp. 249–266, 1972.
- [28] Chimento, F., Caligiana, G. & Mattos, H.C., Modeling the cyclic softening behaviour for the astm a471 steel trough a elasto-plastic continuum approach. *Congresso Nacional em Engenharia Mecanica (CONEM 2000)*, Natal-RN - Brasil, 2000.